



NIH PUBLIC ACCESS

Author Manuscript

J Comput Assist Tomogr. Author manuscript; available in PMC 2011 March 1.

Published in final edited form as:

J Comput Assist Tomogr. 2010 ; 34(2): 163–172. doi:10.1097/RCT.0b013e3181c89d87.

Improved Characterization of Focal Liver Lesions With Liver-Specific Gadoteric Acid Disodium–Enhanced Magnetic Resonance Imaging: A Multicenter Phase 3 Clinical Trial

Steven S. Raman, MD^{*}, Christopher Leary, MD[†], David A. Bluemke, MD[‡], Marco Amendola, MD[§], Dushyant Sahani, MD^{||}, Jeffrey D. McTavish, MD[¶], Jeffrey Brody, MD[#], Eric Outwater, MD^{**}, Donald Mitchell, MD^{††}, Douglas H. Sheafor, MD^{‡‡}, Jeff Fidler, MD^{§§}, Isaac R. Francis, MD^{|||}, Richard C. Semelka, MD^{¶¶}, Kohkan Shamsi, MD, PhD^{##}, Simone Gschwend, MD, PhD^{***}, David R. Feldman, MD^{##}, Josy Breuer, MD^{***}, and United States EOB Study Group

^{*}Department of Radiological Sciences, UCLA, Los Angeles, CA

[†]Hartford Hospital, Hartford, CT

[‡]The Johns Hopkins University School of Medicine, Baltimore, MD

[§]MRI Center, Miami, FL

^{||}Department of Radiology, Massachusetts General Hospital

[¶]Department of Radiology, Brigham and Women's Hospital, Boston, MA

[#]Department of Diagnostic Imaging, Rhode Island Hospital, Providence, RI

^{**}Department of Radiology, University of Arizona Health Sciences Center, Tucson, AZ

^{††}Department of Radiology, Thomas Jefferson University Hospital, Philadelphia, PA

^{‡‡}Department of Radiology, Duke University Medical Center, Durham, NC

^{§§}Department of Radiology, Mayo Clinic, Rochester, MN

^{|||}Department of Radiology, University of Michigan Hospitals, Ann Arbor, MI

^{¶¶}Department of Radiology, University of North Carolina School of Medicine, Chapel Hill, NC

^{##}Bayer HealthCare Pharmaceuticals, Wayne, NJ

^{***}Bayer Schering Pharma AG, Berlin, Germany

Abstract

Objectives—To evaluate the safety of gadoteric acid disodium (Gd-EOB-DTPA) magnetic resonance imaging (MRI) and its efficacy in characterizing liver lesions.

Methods—Lesion characterization and classification using combined (unenhanced and Gd-EOB-DTPA-enhanced) MRI were compared with those using unenhanced MRI and contrast-enhanced

Reprints: Steven S. Raman, MD, Department of Radiological Sciences, UCLA, 10833 Le Conte Ave, Los Angeles, CA 90095-1721 (sraman@mednet.ucla.edu).

Dr Leary is now with Bristol Hospital, Bristol, CT.

Dr Amendola is now with the Main Hospital of Virginia Commonwealth University, Richmond, VA.

Dr McTavish is now with the Hampton Roads Radiology Associates, Norfolk, VA.

spiral computed tomography (CT) using on-site clinical and off-site blinded evaluations for patients with focal liver lesions.

Results—Gadoxetic acid disodium was well tolerated in this study. For the clinical evaluation, more lesions were correctly characterized using combined (unenhanced and Gd-EOB-DTPA-enhanced) MRI than using unenhanced MRI and spiral CT (96% vs 84% and 85%, respectively; $P \leq 0.0008$). For the blinded evaluation, more lesions were correctly characterized using combined MRI compared with using unenhanced MRI (61%–76% vs 48%–65%, respectively; $P \leq 0.0012$ for 2/3 readers); when compared with spiral CT, a similar proportion of lesions were correctly characterized.

Conclusions—Gadoxetic acid disodium-enhanced MRI is of clinical benefit relative to unenhanced MRI and spiral CT for a radiological diagnosis of liver lesions.

Keywords

liver lesion; magnetic resonance; computed tomography; contrast agent; Gd-EOB-DTPA

Improved imaging accuracy in hepatic lesion characterization is crucial for appropriate patient triage. Dynamic contrast-enhanced magnetic resonance imaging (MRI) has remained for more than 10 years as the established technique to characterize detected liver lesions^{1–4}; however, further improvement in lesion detection and characterization would be desirable. Currently approved liver-specific contrast agents, such as ferumoxides and mangafodipir,^{5–7} lack dynamic enhancement information,⁸ and dual contrast-enhanced MRI is cumbersome and not in widespread use.^{9,10}

Gadoxetic acid disodium (Gd-EOB-DTPA: Primovist [Bayer Schering Pharma AG, Berlin, Germany], Eovist [Bayer Healthcare Pharmaceuticals, Wayne, NJ], and EOB-Primovist [Bayer Yakuhin, Osaka, Japan]) is a newly developed liver-specific MRI contrast agent that was first approved in Europe in 2004 and is also approved in many countries of the Asia-Pacific region. More recently, in July 2008, Gd-EOB-DTPA was approved by the Food and Drug Administration in the United States for intravenous use in T1-weighted (TW1) MRI of the liver to detect and characterize lesions in adults with known or suspected focal liver lesions. Gadoxetic acid disodium has extracellular properties similar to conventional Gd-containing extracellular MRI contrast agents but has the additional property of selective hepatocyte uptake, with approximately 50% of the injected dose taken up via the organic anion transporter protein (OATP-1) followed by biliary excretion.^{11–13} Gadoxetic acid disodium also has higher relaxivity rates compared with Gd-DTPA (6.9 L mmol⁻¹ s⁻¹ in plasma at 1.5 T vs 4.1 L mmol⁻¹ s⁻¹ in plasma at 1.5 T).¹⁴ Phase 1 to 3 trials showed good tolerance¹⁵ and improvement in lesion characterization^{16–18} and detection.^{19,20}

Here, we present the findings of a phase 3 trial that, in addition to safety evaluations, was designed to assess whether combined unenhanced and Gd-EOB-DTPA-enhanced MRI improved liver lesion characterization and classification when compared primarily with unenhanced MRI alone and secondarily with dual-phase spiral (helical) computed tomography (CT).

Materials and Methods

Study Design

This open-label, phase 3 study was performed at 18 institutions in the United States. It was an intraindividual comparison of the diagnostic performance of combined unenhanced and Gd-EOB-DTPA-enhanced MRI and the unenhanced MRI or spiral CT to determine liver lesion characterization (lesion-specific diagnosis) and classification (benign/malignant). The

trial protocol was approved by a central ethics committee and 18 local institutional review boards. All participating patients gave informed written consent.

Patients and Liver Lesions

Patients 18 years and older with suspected or known liver lesions who had been referred to have routine CT and MRI were eligible to be included in the trial. A total of 240 patients enrolled in the trial.

Patients were excluded if they could be placed into one of the following categories: underwent liver surgery before MRI, pregnant or breast-feeding mother, previously received Gd-EOB-DTPA or other study drugs within 30 days before MRI, received Gd-DTPA within 24 hours or other liver-specific contrast agent within 2 weeks before MRI, clinically unstable, scheduled for biopsy or surgery within 72 hours of MRI, history of anaphylactoid reactions to medications or contrast media, lack of appropriate standard of reference (SOR) examination, or not adhering to specified time parameters.

Standard of Reference

All lesions or groups of lesions in the study were verified by a predefined, lesion-specific, and ethically justifiable SOR, generally within 3 months of MRI. The following lesion-specific SORs were considered valid if performed within the following timeframes: malignancies, biopsy within 3 months; focal liver fibrosis or fat, biopsy within 12 months; regenerative nodules, biopsy within 4 weeks; adenoma, biopsy within 6 months; focal nodular hyperplasia, biopsy or conventional dynamic contrast-enhanced MRI within 12 months; hemangiomas, conventional dynamic contrast-enhanced MRI or tagged cell scintigraphy (for lesions > 2 cm) within 12 months; liver cysts, sonography within 12 months; hydatid cysts, sonography and serology within 2 weeks; and abscess, aspiration and culture within 2 weeks.

Magnetic Resonance Contrast Agent

Gadoxetic acid disodium is a liver-specific MR contrast agent; its chemical profile, pharmacokinetic properties (hepatocellular uptake via OATP-1 of approximately 50% of the dose), relaxivity rates ($6.9 \text{ L mmo}^{-1} \text{ s}^{-1}$ in plasma at 1.5 T), osmolality, viscosity, and physiological routes of excretion (balanced renal and biliary) have been described previously.^{11–13,15}

The patients received a 25 $\mu\text{mol/kg}$ body weight dose of a 0.25-mol/L solution of Gd-EOB-DTPA (volume range, 4.0–12.0 mL), which was bolus injected at 2 mL/s through a cubital intravenous line and then flushed with 30 mL of 0.9% saline.

Safety Evaluation

The patients were observed and evaluated for adverse events (AEs) for 72 hours after the administration of Gd-EOB-DTPA. All subjective and objective AEs were recorded. Vital signs, 12-lead electrocardiograms, and clinical laboratory tests (hematological, coagulation, and clinical chemistry tests and urinalysis) were obtained at multiple time points in all the patients.

Magnetic Resonance Imaging

Magnetic resonance imaging was performed using the 1.5-T MR Systems with phased array surface coils. Each patient first underwent the following precontrast sequences: T2W fast spin echo (FSE)/turbo spin echo/single-shot FSE/half-Fourier acquisition single-shot turbo spin-echo sequence (repetition time, ≥ 2000 milliseconds; echo time, 90–120 milliseconds;

number of excitations, 1–4; matrix, 192–256 × 256; slice thickness, 5–8 mm; gap, 0–2 mm; breath hold and fat suppression, optional) and T1W 2-dimensional gradient-recalled echo (GRE) fast low-angle shot (FLASH) sequence with and without chemically selective fat suppression (repetition time, 100–200 milliseconds; echo time, ≤8 milliseconds; matrix, 128–256 × 256; slice thickness, 5–8 mm; gap, 0–2 mm). After completion of the intravenous injection of Gd-EOB-DTPA, breath-hold 2-dimensional GRE/FLASH T1 sequences in the arterial (10–20 seconds), portovenous (50–60 seconds), and equilibrium phases (100–120 seconds) were acquired. The T2W and T1W sequences were repeated 20 minutes after Gd-EOB-DTPA injection.

Computed Tomography

Biphasic spiral CT was performed on predominantly single-detector scanners (100 to 150 kV; 180–300 mAs; pitch, 1 to 2; and slice thickness and reconstruction interval, 5 to 7 mm). Using a power injector, 3 to 5 mL/s (100–200 mL) of iodinated, nonionic contrast material was administered intravenously. Hepatic arterial and portal venous phase imagings were performed after a delay of 25 to 35 seconds and 45 to 70 seconds, respectively, after the start of contrast injection.

Image Evaluation

The MR and CT images were reviewed either unblindedly on site by one experienced clinical investigator per study site to mimic routine clinical practice or blindedly off site by 3 experienced abdominal image radiologists (readers 1, 2, and 3) who were not involved in the unblinded image review (blinded off-site evaluations were performed by a central core laboratory).

Lesion Identification

For correct lesion identification and to eliminate confusion in cases with multiple lesions, each SOR-proven lesion was marked on both the MR and CT images by the clinical investigator and assigned a unique number, which was used throughout the study on all imaging sequences.

Image Evaluation in the Clinical Study

For all MR images, the clinical investigator first assessed the T1W and T2W unenhanced images followed by the combined MR sequences (unenhanced images, T1W dynamic enhanced images, T1W delayed hepatocyte-specific images, and postcontrast T2W images). Each clinical investigator separately assessed the images from the dual-phase spiral CT. They recorded their evaluations with respect to characterization, classification, and confidence during the prospective reading in a detailed modality-specific record.

Image Evaluation in the Blinded Off-Site Review

The off-site evaluation was performed in 3 sessions separated by two 3-week intervals to minimize recall and memory bias. The readers were blinded to the patient-related information, the imaging technique, and the contrast information. During the first session, the readers evaluated all the unenhanced images (T1W and T2W) separately from the enhanced images (T1W dynamic, T1W delayed hepatocyte-specific images, and postcontrast T2W images) in a random patient order. In the second session, the combined MR images (unenhanced and dynamic and delayed) were evaluated. The dual-phase spiral CT images were reviewed during the third session. Each reader assessed every image for all the patients.

In both the on-site clinical and off-site blinded evaluations, the primary end point was the performance of combined MRI (unenhanced and Gd-EOB-DTPA-enhanced) compared with unenhanced MRI in characterizing focal lesions (as measured by the proportion of detected lesions with correct characterization). This intended to reflect real-life clinical practice because both unenhanced and enhanced MR images are used together for evaluation of lesions in clinical practice. Correct lesion characterization was achieved when radiological interpretation agreed with the SOR diagnosis.

Secondary end points included the comparison of the performance of combined MRI versus spiral CT in characterizing focal liver lesions in both the on-site clinical and off-site blinded evaluations and the comparison of the characterization performance of Gd-EOB-DTPA-enhanced MRI (dynamic and delayed hepatocyte-specific images [20 minutes after administration]) versus unenhanced MRI only in the blinded evaluation.

The clinical and blinded readers graded the confidence of characterization for each lesion on a 5-point scale for unenhanced MRI, combined MRI, and spiral CT data. A score of 1 indicated low or doubtful confidence that lesion morphology and enhancement were characteristic of a specific lesion type, whereas a score of 5 indicated highest confidence that the spiral CT and MRI features were characteristic of specific lesion types.

Analysis of discordant lesions, defined as those correctly characterized by one modality but incorrectly characterized by another modality, was performed in the clinical and blinded reviews.

Both the unblinded clinical on-site and blinded off-site readers classified each representative lesion as malignant, benign, or not assessable during the review of images from the unenhanced and combined MRI and CT. The readers also scored the confidence of classification of each individual lesion based on standard radiological signs on a 5-point scale, where 1 indicated low or doubtful confidence and 5 indicated complete confidence that the radiological features ascribed to the lesion were representative of each lesion category.

Accuracy, sensitivity, and specificity of lesion classification were calculated separately for spiral CT and for enhanced, unenhanced, and combined MRI compared with the SOR. Because the SOR was defined as the criterion standard, the assessment “not assessable” was not accepted as a result of the reference standard.

Statistical Analysis

The primary objectives were to calculate the proportion of detected lesions with correct characterization (lesion diagnosis) on combined MRI or enhanced MRI compared with that on unenhanced MRI and to show superiority. Performance in lesion characterization was evaluated on a per-lesion basis for each patient and for all the patients. Because some patients may have had multiple lesions detected and verified by the SOR, an adjustment of the 2-tailed McNemar test of paired proportions, proposed by Eliasziw and Donner²¹ to take into account clustering, was used for this hypothesis test at a 5% significance level.

Results

Of the 240 patients enrolled in the trial, 5 did not receive intravenous Gd-EOB-DTPA. A total of 197 patients had a valid lesion-specific SOR; however, 20 had protocol deviations and were excluded from the efficacy analysis. Thus, 177 patients were eligible to be included in the efficacy analysis. All 235 patients who received Gd-EOB-DTPA were

included in the safety analysis. There were 124 men (53%) and 111 women (47%) with the mean age of 54.2 years (range, 22–81 years).

Safety of Gd-EOB-DTPA

The contrast medium was well tolerated by patients. Fifty-two AEs occurred in 39 (16.6%) of the 235 patients after administration of a contrast injection, of which 14 AEs in 12 patients (5.1%) were considered by the investigator to be possibly or probably drug related. None were considered definitely related to the study drug by the investigator. Adverse events considered possibly or probably related to the study drug were taste perversion (4 patients), headache (2 patients), vasodilatation (1 patient), nausea (1 patient), bundle branch block (1 patient), rash (1 patient), maculopapular rash (1 patient), dizziness (1 patient), diarrhea (1 patient), and dry mouth (1 patient). No patients discontinued the study. There were no clinically relevant changes in the clinical, electrocardiogram, or laboratory parameters in any patients.

Efficacy

A total of 269 lesions with an SOR in 177 patients were included for efficacy analysis, of which 92 lesions were malignant and 177 were benign. The primary malignancies consisted of 38 patients with hepatocellular carcinoma, 4 patients with cholangiocarcinomas, and 2 patients with focal lymphomas. Most liver metastases originated from colorectal, gastric, or pancreatic adenocarcinomas (44/48 patients).

The benign lesions consisted of 67 hemangiomas, 37 focal nodular hyperplasias, 54 simple cysts, 10 focal fat, 4 regenerative nodules, 2 adenomas, 1 abscess, and 1 bile duct adenoma, and one patient had only normal liver tissue and no lesion.

On-site Evaluation (Clinical Study)

Primary Evaluation—In 177 patients, the proportion of correctly characterized lesions was significantly higher using combined MRI (96%) compared with either unenhanced MRI (84%; $P = 0.0002$) or spiral CT (85%; $P = 0.0008$; Table 1).

The number of patients evaluated for the primary end point was different to the number of patients evaluated for the comparison of MRI and spiral CT because in some patients, spiral CT was not performed or was not performed within 6 weeks of MRI.

Secondary Evaluation—Of the discordant lesions, 11.5% (31/269) were correctly characterized using combined MRI but incorrectly characterized using unenhanced MRI, whereas only 0.4% (1/269) were correctly characterized using unenhanced MRI alone. In comparison, 11.9% (31/261) of the lesions were correctly characterized by combined MRI but incorrectly characterized by spiral CT; a total of 1.1% (3/261) of the lesions were correctly characterized by spiral CT alone.

When assessing the confidence of lesion characterization, a greater proportion of lesions were assigned with high confidence (4 or 5) with combined MRI compared with that with spiral CT or unenhanced MRI (92% [236/269 lesions] versus 62% [140/269 lesions] or 79% [174/221 lesions], respectively; Table 2).

The proportion of lesions with a correct classification (benign or malignant) was also highest for combined MRI (98% [264/269 lesions]), relative to unenhanced MRI (92% [247/269 lesions]) or spiral CT (88% [230/261 lesions]). The highest confidence of classification scores (4 or 5) were reported using combined MRI (94% [246/262]) compared with

unenanced MRI (66% [155/235]) and spiral CT (81% [185/227]). Sensitivity, specificity, and accuracy were all highest for combined MRI (Table 3).

Off-site Blinded Evaluation

Primary Evaluation—All 3 blinded readers correctly characterized more lesions using combined MRI relative to unenanced MRI. The proportion of correctly characterized lesions increased by 1%, 11%, and 19% for readers 1, 2, and 3, respectively, with significant improvement ($P \leq 0.0012$) for 2 of 3 readers (Table 4; Figs. 1–3).

Secondary Evaluation—All the readers correctly characterized a greater proportion of the lesions using enhanced MR sequences compared with unenanced MR sequences (significant for 2 of the 3 readers; reader 1, $P = 0.859$; reader 2, $P = 0.0001$; reader 3, $P = 0.0002$; Table 5, enhanced sequences vs unenanced sequences). Similarly, all the readers correctly characterized a greater proportion of the lesions using combined MR images compared with dual-phase spiral CT (not significantly different for any of the readers; Table 5, combined MRI vs spiral CT).

Of the discordant lesions, all the readers correctly characterized more lesions using combined or enhanced MRI (Tables 6) relative to unenanced MRI or spiral CT. Conversely, fewer lesions were correctly characterized using unenanced MRI or spiral CT than on enhanced or combined MRI. Confidence of characterization was highest for all readers on combined MR sequences (Table 7).

In analysis of lesion classification as benign or malignant, most readers (2 of 3) correctly classified more lesions using combined MRI relative to unenanced MRI (77% vs 78%, 89% vs 87%, and 85% vs 79% for readers 1, 2, and 3, respectively), and all the readers correctly classified more lesions using combined MRI relative to spiral CT (65%, 82%, and 77% for readers 1, 2, and 3, respectively; Table 8), with highest confidence using combined MRI (75%–98%, 69%–78%, and 64%–89% for combined MRI, unenanced MRI, and spiral CT, respectively; Table 9).

For the blinded analysis, when comparing combined MRI with unenanced MRI, sensitivity and accuracy for lesion classification increased slightly for 2 of 3 readers (sensitivity: 96% vs 93%, 97% vs 94%, and 80% vs 87%; accuracy: 79% vs 79%, 89% vs 88%, and 83% vs 80%, for readers 1, 2, and 3, respectively); specificity increased for 1 of the 3 readers and was unchanged for the 2 other readers (67% vs 67%, 83% vs 83%, and 83% vs 80% for readers 1, 2, and 3, respectively). The accuracy for lesion classification was highest in combined MRI compared with spiral CT for all readers (Table 10).

Discussion

Most of the previously published studies that have determined the accuracy of MRI have focused on lesion detection as a primary end point with variable rigorousness of lesion verification.^{22–24} However, for maximal clinical utility, improved detection, classification, and characterization of lesions are necessary for widespread use of any liver agent because clinical therapy decisions rely on the knowledge of malignancy and the diagnosis of a specific lesion type. Our study was specifically designed to assess the diagnostic performance for the classification and characterization of focal liver lesions using combined MRI using the liver-specific contrast agent, Gd-EOB-DTPA.

With Gd-EOB-DTPA-enhanced MRI, both dynamic enhancement information (such as conventional Gd-DTPA-enhanced MRI)²⁵ and delayed (20 minutes) T1 hepatocyte-specific enhancement (such as manganese dipyridoxal diphosphate)⁷ are obtained. Superior lesion

detection was shown in recent multi-center trials using Gd-EOB-DTPA-enhanced MRI when compared with unenhanced MRI.^{19,20} Sensitivity was higher, and fewer false-positive lesions resulted with Gd-EOB-DTPA-enhanced MRI compared with spiral CT, especially when lesions less than 1 cm were considered.¹⁸ However, large multicenter studies are needed to evaluate the value of Gd-EOB-DTPA-enhanced MRI for characterization of focal liver lesions.

Here, we report a phase 3, multicenter trial conducted in the United States, where a 1.5-T MRI was used to determine whether Gd-EOB-DTPA-enhanced MRI improved hepatic lesion characterization and classification both clinically and in independent, blinded reader evaluation relative to unenhanced scans and, secondarily, to standard dual-phase spiral CT. A wide variety of rigorously proven benign and malignant lesions were imaged.

In both the clinical and blinded evaluations, in comparison with unenhanced MR images, combined unenhanced and Gd-EOB-DTPA-enhanced MRI significantly improved focal hepatic lesion characterization. In the blinded reading, a secondary comparison of enhanced and unenhanced sequences showed that all the 3 readers improved lesion characterization performance when enhanced sequences were used. Furthermore, in both the clinical and blinded evaluations, the combined MRI enabled the best lesion classification (benign or malignant) and improved confidence of classification compared with the unenhanced MRI and the spiral CT in both evaluations.

In these analyses, the combined MR sequences allowed improved characterization compared with the spiral CT, as shown by the primary evaluation and the discordant lesion evaluation. The difference was larger in the clinical study because of its unblinded nature, which either reflects true clinical practice or may indicate bias where additional information often influences radiological interpretations.^{26–28}

In addition to the objective parameters, which included the proportion of correctly characterized lesions or any sensitivity and specificity calculation, the evaluation of the confidence in characterization is an important supportive parameter for the performance of an imaging method because triage to further radiological investigations, biopsy, or therapy is influenced by the degree of radiological confidence. In both evaluations, combined MRI had the highest confidence scores with respect to lesion characterization, which is clinically important because the radiologist's confidence impacts further patient management.

Limitations regarding the study design have been considered. Not all benign lesions (15.6% [31/199]) had histological proof as SOR because biopsies of benign liver lesions, such as hemangiomas or focal nodular hyperplasia, were not the standard of care and therefore not ethically justifiable. In addition, we did not subanalyze the utility of each individual enhancement phase and thus did not address the relative value of the dynamic and hepatocyte-specific phases.

In summary, Gd-EOB-DTPA-enhanced MRI is safe and significantly improves the ability to characterize and classify a variety of focal hepatic lesions relative to unenhanced MRI and dual-phase spiral CT.

Acknowledgments

The authors thank Celia J. Parkyn, PhD, Medicus International, for her editorial assistance. The blinded readings were performed by P. Bret, Department of Medical Imaging, Toronto, Canada; King C. Li, Diagnostic Radiology, Warren Grant Magnuson Clinical Center, Bethesda, Md; and J. Heiken, Department of Radiology, Mallinckrodt Institute of Radiology, St Louis, Mo.

Funding of this study and its editorial support were received from and sponsored by Bayer Schering Pharma AG, Berlin, Germany.

References

1. Hamm B, Thoeni RF, Gould RG, et al. Focal liver lesions: characterization with nonenhanced and dynamic contrast material-enhanced MR imaging. *Radiology* 1994;190:417–423. [PubMed: 8284392]
2. Mitchell DG, Saini S, Weinreb J, et al. Hepatic metastases and cavernous hemangiomas: distinction with standard- and triple-dose gadoteridol-enhanced MR imaging. *Radiology* 1994;193:49–57. [PubMed: 8090921]
3. Petersein J, Spinazzi A, Giovagnoni A, et al. Focal liver lesions: evaluation of the efficacy of gadobenate dimeglumine in MR imaging—a multicenter phase III clinical study. *Radiology* 2000;215:727–736. [PubMed: 10831691]
4. Whitney WS, Herfkens RJ, Jeffrey RB, et al. Dynamic breath-hold multiplanar spoiled gradient-recalled MR imaging with gadolinium enhancement for differentiating hepatic hemangiomas from malignancies at 1.5 T. *Radiology* 1993;189:863–870. [PubMed: 8234717]
5. Federle M, Chezmar J, Rubin DL, et al. Efficacy and safety of mangafodipir trisodium (MnDPDP) injection for hepatic MRI in adults: results of the U.S. Multicenter phase III clinical trials. Efficacy of early imaging. *J Magn Reson Imaging* 2000;12:689–701. [PubMed: 11050638]
6. Ros PR, Freeny PC, Harms SE, et al. Hepatic MR imaging with ferumoxides: a multicenter clinical trial of the safety and efficacy in the detection of focal hepatic lesions. *Radiology* 1995;196:481–488. [PubMed: 7617864]
7. Torres CG, Lundby B, Sterud AT, et al. MnDPDP for MR imaging of the liver. Results from the European phase III studies. *Acta Radiol* 1997;38:631–637. [PubMed: 9245956]
8. Paley MR, Mergo PJ, Torres GM, et al. Characterization of focal hepatic lesions with ferumoxides-enhanced T2-weighted MR imaging. *AJR Am J Roentgenol* 2000;175:159–163. [PubMed: 10882267]
9. Semelka RC, Helmberger TK. Contrast agents for MR imaging of the liver. *Radiology* 2001;218:27–38. [PubMed: 11152776]
10. Ward J, Guthrie JA, Scott DJ, et al. Hepatocellular carcinoma in the cirrhotic liver: double-contrast MR imaging for diagnosis. *Radiology* 2000;216:154–162. [PubMed: 10887242]
11. Clement O, Muhler A, Vexler V, et al. Gadolinium-ethoxybenzyl-DTPA, a new liver-specific magnetic resonance contrast agent. Kinetic and enhancement patterns in normal and cholestatic rats. *Invest Radiol* 1992;27:612–619. [PubMed: 1428739]
12. Schuhmann-Giampieri G, Schmitt-Willich H, Press WR, et al. Preclinical evaluation of Gd-EOB-DTPA as a contrast agent in MR imaging of the hepatobiliary system. *Radiology* 1992;183:59–64. [PubMed: 1549695]
13. Weinmann HJ, Schuhmann-Giampieri G, Schmitt-Willich H, et al. A new lipophilic gadolinium chelate as a tissue-specific contrast medium for MRI. *Magn Reson Med* 1991;22:233–237. Discussion 242. [PubMed: 1812351]
14. Rohrer M, Bauer H, Mintorovitch J, et al. Comparison of magnetic properties of MRI contrast media solutions at different magnetic field strengths. *Invest Radiol* 2005;40:715–724. [PubMed: 16230904]
15. Hamm B, Staks T, Muhler A, et al. Phase I clinical evaluation of Gd-EOB-DTPA as a hepatobiliary MR contrast agent: safety, pharmacokinetics, and MR imaging. *Radiology* 1995;195:785–792. [PubMed: 7754011]
16. Halavaara J, Breuer J, Ayuso C, et al. Liver tumor characterization: comparison between liver-specific gadoxetic acid disodium-enhanced MRI and biphasic CT—a multicenter trial. *J Comput Assist Tomogr* 2006;30:345–354. [PubMed: 16778605]
17. Reimer P, Rummeny EJ, Shamsi K, et al. Phase II clinical evaluation of Gd-EOB-DTPA: dose, safety aspects, and pulse sequence. *Radiology* 1996;199:177–183. [PubMed: 8633143]

18. Hammerstingl R, Huppertz A, Breuer J, et al. Diagnostic efficacy of gadoxetic acid (Primovist)-enhanced MRI and spiral CT for a therapeutic strategy: comparison with intraoperative and histopathologic findings in focal liver lesions. *Eur Radiol* 2008;18:457-467. [PubMed: 18058107]
19. Bluemke DA, Sahani D, Amendola M, et al. Efficacy and safety of MR imaging with liver-specific contrast agent: U.S. multicenter phase III study. *Radiology* 2005;237:89-98. [PubMed: 16126918]
20. Huppertz A, Balzer T, Blakeborough A, et al. Improved detection of focal liver lesions at MR imaging: multicenter comparison of gadoxetic acid-enhanced MR images with intraoperative findings. *Radiology* 2004;230:266-275. [PubMed: 14695400]
21. Eliasziw M, Donner A. Application of the McNemar test to non-independent matched pair data. *Stat Med* 1991;10:1981-1991. [PubMed: 1805322]
22. Heiken JP, Weyman PJ, Lee JK, et al. Detection of focal hepatic masses: prospective evaluation with CT, delayed CT, CT during arterial portography, and MR imaging. *Radiology* 1989;171:47-51. [PubMed: 2538862]
23. Kondo S, Katoh H, Shimizu T, et al. Preoperative embolization of the common hepatic artery in preparation for radical pancreatectomy for pancreas body cancer. *Hepatogastroenterology* 2000;47:1447-1449. [PubMed: 11100373]
24. Wernecke K, Rummeny E, Bongartz G, et al. Detection of hepatic masses in patients with carcinoma: comparative sensitivities of sonography, CT, and MR imaging. *AJR Am J Roentgenol* 1991;157:731-739. [PubMed: 1892027]
25. Vogl TJ, Kummel S, Hammerstingl R, et al. Liver tumors: comparison of MR imaging with Gd-EOB-DTPA and Gd-DTPA. *Radiology* 1996;200:59-67. [PubMed: 8657946]
26. Baker ME, Pelley R. Hepatic metastases: basic principles and implications for radiologists. *Radiology* 1995;197:329-337. [PubMed: 7480672]
27. Nagao T, Inoue S, Goto S, et al. Hepatic resection for hepatocellular carcinoma. Clinical features and long-term prognosis. *Ann Surg* 1987;205:33-40. [PubMed: 3026259]
28. Sugarbaker PH. Surgical decision making for large bowel cancer metastatic to the liver. *Radiology* 1990;174:621-626. [PubMed: 2406776]

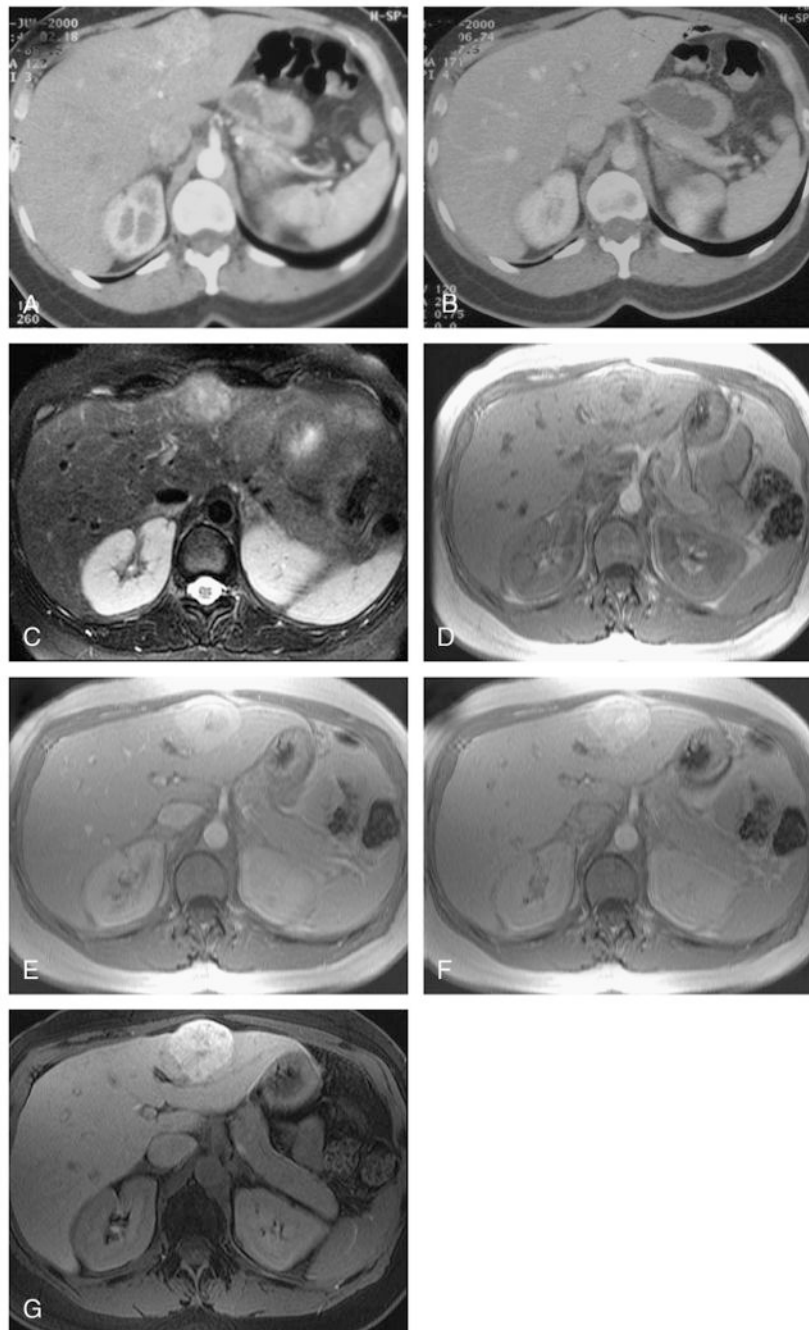


FIGURE 1.

Focal nodular hyperplasia in a female patient aged 47 years. Using dual-phase helical CT, a segment 2 lesion enhances avidly in the arterial phase (A) and becomes isodense to the liver in the portal venous phase (B). No discrete scar was present on this or several other similar lesions (not shown), and the lesions were incorrectly interpreted as hypervascular metastases on blinded reading. Using unenhanced MRI, the lesion was of intermediate hyperintensity on the T2W images with hyperintense central scar (C) and mild hyperintensity on the T1W images (D). Using dynamic Gd-EOB-DTPA-enhanced sequences, the lesions also enhanced avidly in the late arterial phase (E) with enhancement of the central scar in the portal venous phases (F). At 20 minutes after injection, the hepatocellular lesion retains contrast (G). The

other lesions also showed similar characteristics and were correctly interpreted as focal nodular hyperplasia on blinded reading of combined images.

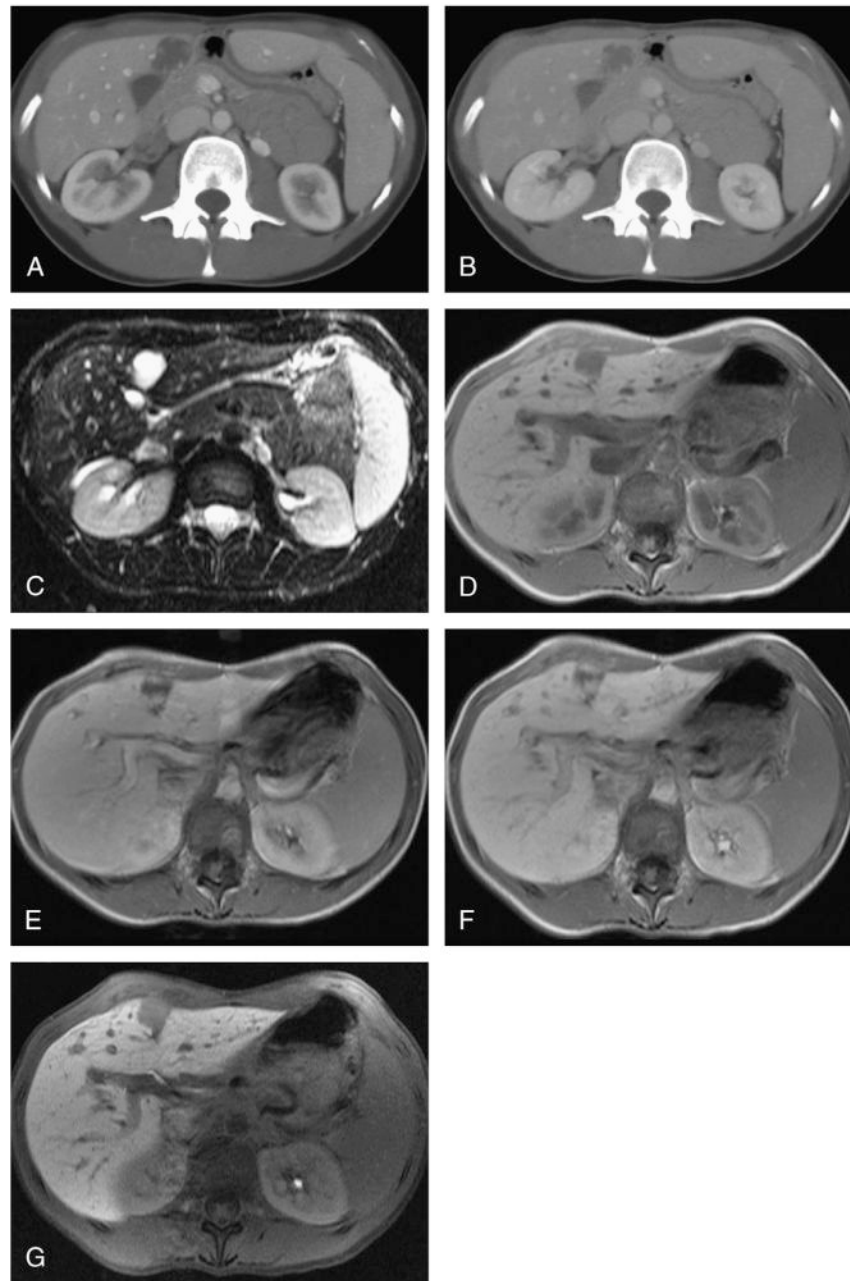


FIGURE 2.

Hemangiomas in a female patient aged 30 years. Using dual-phase helical CT, nodular peripheral enhancement is present in a segment 4 lesion in the arterial phase (A) with progressive enhancement in the portal venous phase (B). Other similar lesions (not shown) were present with similar features, and the lesions were interpreted as hemangiomas on blinded reading. Using unenhanced MRI, the lesion was uniformly and markedly hyperintense on T2W images (C) and hypointense on T1W images (D) and interpreted as a simple cyst. Using dynamic Gd-EOB-DTPA-enhanced sequences, the lesions also showed characteristic progressive nodular peripheral enhancement in the late arterial (E) and portal venous phases (F). At 20 minutes after injection, the lesion signal has decreased in

comparison with the background liver (G). Based on combined images, the lesions were interpreted as hemangiomas.

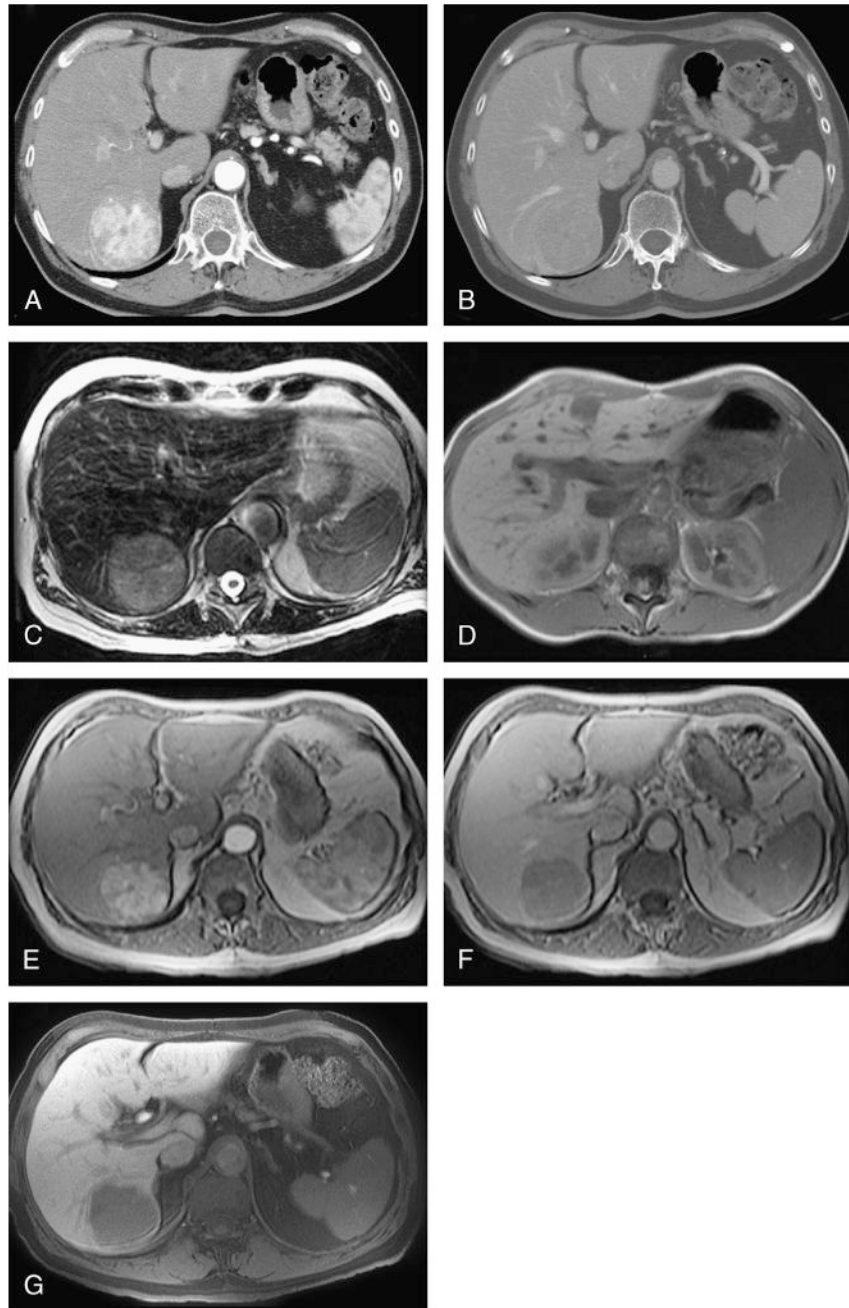


FIGURE 3. Hepatocellular carcinoma in a male patient aged 75 years with proven histopathology. Using dual-phase helical CT, a segment 7 mass markedly enhances compared with the liver (A) and then rapidly becomes isointense with capsular enhancement in the portal venous phase (B). The mass was interpreted as a hepatocellular carcinoma on blinded reading. On unenhanced MRI, the mass was of intermediate hyperintensity on the T2W images (C) and hypointense on the T1W images (D) and interpreted as a hemangioma. Using dynamic Gd-EOB-DTPA-enhanced sequences, the mass enhanced avidly relative to liver late arterial phase (E) and then unenhanced with delayed capsular enhancement in the late portal venous phase (F). At 20 minutes after injection, the lesion signal was hypointense in comparison to

the background liver (G). Using combined images, the lesion was interpreted as a hepatocellular carcinoma. Overall confidence of characterization was stronger for combined images relative to the CT images alone.

TABLE 1
Clinical Evaluation: Proportion of Correctly Characterized Lesions

	Correctly Characterized Lesions, n (%)	95% Confidence Interval	<i>P</i> *
Combined MRI [†] (n = 269 lesions)	257 (96)	—	—
Unenhanced MRI (n = 269 lesions)	227 (84)	0.055–0.167	0.0002
Spiral CT (n = 261 lesions)	222 (85)	0.047–0.167	0.0008

* *P* value versus combined MRI.

[†] Combination of unenhanced and enhanced MR sequences.

TABLE 2
Clinical Evaluation: Confidence of Lesion Characterization

Imaging Technique	Percentage of Lesions Assigned 4 or 5, n (%)
Combined MRI† (n = 269 lesions)	236 (92)
Unenhanced MRI (n = 269 lesions)	140 (62)
Spiral CT (n = 221 lesions)	174 (79)

Confidence of lesion characterization was defined using a 5-point scale: 1 indicates low or doubtful confidence, whereas 5 indicates high or complete/almost complete confidence. Combination of unenhanced and enhanced MR sequences.

TABLE 3
Clinical Evaluation: Test Parameters for Lesion Classification (Benign/Malignant)
Comparing Combined MRI With Unenhanced MR and Spiral CT

	Combined MRI (n = 269 Lesions)	Unenhanced MRI (n = 269 Lesions)	Spiral CT (n = 261 Lesions)
TP, n (%)	93 (35)	85 (32)	77 (30)
TN, n (%)	171 (64)	162 (60)	153 (59)
FP, n (%)	4 (1)	13 (5)	17 (7)
FN, n (%)	1 (<0)	9 (3)	14 (5)
Sensitivity, %	99.4	90	89.3
Specificity, %	96.0	91.8	88.9
Accuracy, %	97.5	90.9	89.1

Includes only lesions verified by SOR.

FN indicates false negatives (benign, no lesion, or not assessable in the imaging procedure but malignant in SOR); FP, false positives (malignant or not assessable in the imaging procedure but benign or no lesion in the SOR); TN, true negatives (benign or no lesion in the imaging procedure and in SOR); TP, true positives (malignant in the imaging procedure and in the SOR)

TABLE 4
Blinded Evaluation: Primary Analysis of the Proportion of Correctly Characterized Lesions Using Combined MR Sequences Versus Unenhanced Sequences

Reader	Combined MRI, (n = 269 Lesions), n (%)	Unenhanced MRI, (n = 269 Lesions), n (%)	<i>P</i>
1	163 (61)	161 (60)	0.859
2	204 (76)	174 (65)	0.0012
3	180 (67)	129 (48)	≤0.0001

TABLE 5
Blinded Evaluation: Secondary Analysis of the Proportion of Correctly Characterized Lesions

Reader	Enhanced MRI (n = 269 Lesions), n (%)	Unenhanced MRI (n = 269 Lesions), n (%)	P
1	168 (62)	161 (60)	0.859
2	210 (78)	174 (65)	0.0001
3	175 (66)	129 (48)	0.0002
	Combined MRI, n (%)	Spiral CT, n (%)	P
1 (n = 254 lesions)	157 (62)	146 (57)	0.4361
2 (n = 250 lesions)	193 (77)	189 (76)	0.6329
3 (n = 250 lesions)	165 (66)	161 (64)	0.6342

TABLE 6
Blinded Evaluation: Proportion of the Discordant Lesions

Reader	Characterized Correctly Using Combined MRI but Incorrect Using Unenhanced MRI (n = 269 lesions), n (%)	Characterized Correctly Using Unenhanced MRI but Incorrect Using Combined MRI (n = 269 lesions), n (%)
1	34 (12.6)	32 (12.0)
2	46 (17.1)	16 (6.0)
3	66 (24.5)	15 (6.0)
Reader	Characterized Correctly Using Enhanced MRI but Incorrectly Using Unenhanced MRI (n = 269 lesions), n (%)	Characterized Correctly Using Unenhanced MRI but Incorrectly Using Enhanced MRI (n = 269 lesion), n (%)
1	37 (13.8)	30 (11)
2	46 (17.1)	10 (4)
3	61 (22.7)	15 (6)
Reader	Characterized Correctly Using Combined MRI but Incorrectly Using Spiral CT, n (%)	Characterized Correctly Using Spiral CT but Incorrectly Using Combined MRI, n (%)
1 (n = 254 lesions)	48 (18.9)	37 (15)
2 (n = 250 lesions)	29 (11.6)	25 (10)
3 (n = 250 lesions)	32 (12.8)	28 (11)

TABLE 7
Confidence of Characterization in the Blinded Evaluation: Proportion of Lesions Assigned a Score of 4 or 5

Reader	Combined MRI, n (%)	Unenhanced MRI, n (%)	Spiral CT, n (%)
1	158/163 (97)	118/160 (74)	127/146 (87)
2	159/204 (78)	101/173 (59)	119/188 (63)
3	133/180 (74)	92/129 (71)	107/160 (67)

Confidence of lesion characterization was defined using a 5-point scale: 1 indicates low or doubtful confidence, whereas 5 indicates high or complete/almost complete confidence.

TABLE 8
Blinded Evaluation: Proportion of Correctly Classified SOR-Verified Lesions

Reader	Enhanced MRI (n = 269), n (%)	Combined MRI (n = 269), n (%)	Unenhanced MRI (n = 269), n (%)	Spiral CT (n = 261), n (%)
1	207 (77)	208 (77)	210 (78)	175 (65)
2	241 (90)	239 (89)	234 (87)	221 (82)
3	226 (84)	228 (85)	212 (79)	206 (77)

TABLE 9
Confidence of Classification in the Blinded Evaluation: Proportion of Lesions Assigned a Score of 4 or 5

Reader	Combined MRI n (%)	Unenhanced MRI n (%)	Spiral CT n (%)
1	204/208 (98)	158/208 (76)	156/175 (89)
2	184/239 (77)	152/222 (69)	140/219 (64)
3	167/223 (75)	156/200 (78)	137/203 (68)

Confidence of lesion characterization was defined using a 5-point scale: 1 indicates low or doubtful confidence, whereas 5 indicates high or complete/almost complete confidence.

TABLE 10
Sensitivity, Specificity, and Accuracy for Lesion Classification

	Enhanced MRI (n = 269), Reader 1/2/3, %	Combined MRI (n = 269), Reader 1/2/3, %	Unenhanced MRI (n = 269), Reader 1/2/3, %	Spiral CT (n = 250), Reader 1/2/3, %
Blinded evaluation: raw data for calculating test parameters*				
TP	34/34/32	33/33/29	33/33/30	33/29/29
TN	43/56/52	44/55/56	45/54/49	36/60/54
FP	22/9/13	21/10/9	20/11/16	29/6/11
FN	1/1/3	1/1/6	2/2/4	2/6/7
Test parameter percentages for lesion classification (benign/malignant) comparing unenhanced MRI with combined MRI, enhanced MRI, or spiral CT in the blinded evaluation				
Blinded study				
Sensitivity	97/98/90	96/97/80	93/94/87	94/83/82
Specificity	62/85/76	67/83/84	67/83/74	55/88/80
Accuracy	78/91/82	79/89/83	79/88/80	72/86/81

* Includes only lesions verified by SOR.